MODELLING AND PARAMETRIC PERFORMANCE ANALYSIS OF AN AEM ELECTROLYSER USING ASPEN PLUS

A B.Tech. Project I Report Submitted in partial fulfilment of the requirements for the degree of Bachelor of Technology

by

Ankit Saha

22CH30004

Under the guidance of

Dr. Sourav Mondal

DEPARTMENT OF CHEMICAL ENGINEERING

INDIAN INSTITUTE OF TECHNOLOGY

KHARAGPUR – 721302

NOVEMBER 2025

DECLARATION

I affirm that:

a. The contents of this report represent my own work, carried out under the supervision of my project guide.

b. Any external information utilized in this report has been properly acknowledged through citations and listed in the reference section.

c. I have prepared this document in accordance with the reporting instructions issued by the Institute.

d. I have complied with all rules and principles outlined in the Institute's Ethical Code of Conduct throughout the preparation of this work.

e. This report, in full or in part, has not been submitted to any other institute or university towards any academic award.

Ankit Saha

22CH30004

CERTIFICATE

This is to certify that the work embodied in this project report, titled "MODELLING AND PARAMETRIC PERFORMANCE ANALYSIS OF AN AEM ELECTROLYSER USING ASPEN PLUS," has been carried out by Ankit Saha (22CH30004) under my supervision.

The report is approved for submission.

Date: Signature of Supervisor

ACKNOWLEDGEMENT

I would like to acknowledge and express my heartfelt gratitude to my thesis supervisor, *Dr. Sourav Mondal,* who made this work possible through his enthusiasm and unwavering encouragement throughout the project. His direction and guidance guided me through all phases of completion of this thesis.

I would also like to extend my sincere gratitude to *Mr. Rajeev Ranjan* (Research Scholar, Department of Chemical Engineering) for their invaluable guidance and insightful discussions. Their support and mentorship were instrumental in the successful completion of this project.

To my parents, for your trust, for providing unwavering support and motivation throughout my dedication to my thesis work.

Abstract :

The growing integration of renewable energy into power systems has increased the need for reliable long-duration energy storage technologies. Hydrogen production through water electrolysis is a promising solution, and Anion Exchange Membrane (AEM) electrolysers, in particular, offer a cost-effective and environmentally benign alternative to conventional alkaline. In this project, a zero-gap AEM electrolyser was modelled using Aspen Plus by adapting the semi-empirical voltage formulation originally developed for alkaline water electrolysers (AWE). The model incorporates reversible thermodynamics, activation behaviour, ohmic resistance, and concentration effects, enabling a realistic representation of AEM operating conditions.

A base-case electrolyser model was validated against experimental polarization data, showing strong agreement across the full current density range. A comprehensive parametric analysis was then performed to examine the influence of temperature, electrolyte concentration, membrane thickness, and electrode exchange current densities on cell performance. The results show that increasing temperature and electrolyte concentration significantly lowers cell voltage due to improved kinetics and ionic conductivity. Thinner membranes reduce ohmic losses, while both anode and cathode exchange current densities strongly affect activation overpotentials, with the anode showing greater sensitivity. Additional parameters such as feed flow rate and anode-to-feed ratio were found to have negligible influence on performance.

Overall, this work demonstrates that Aspen Plus can effectively model AEM electrolyser behaviour using an adapted AWE framework and provides clear insights into key operating factors that govern efficiency and voltage losses. The findings can support design optimisation and further development of AEM systems for green hydrogen production.

Introduction:

The global shift toward renewable energy has increased interest in hydrogen as a clean and efficient energy carrier. Hydrogen is particularly valuable for large-scale and long-duration energy storage, helping to overcome the intermittency of solar and wind power, which conventional batteries cannot easily manage. Among water electrolysis technologies, Alkaline Water Electrolyzers (AWE) are well-established and cost-effective but face limitations such as lower current densities and gas crossover due to the use of liquid electrolytes and corrosion due to the high concentration of KOH. Anion Exchange Membrane (AEM) electrolysers have recently emerged as a promising alternative, offering the advantages of alkaline operation while using a solid polymer membrane, which enables higher efficiency and reduced material costs.

AEM electrolysers allow the use of non-precious catalysts, enhance gas separation, and provide flexibility for decentralised hydrogen production and renewable energy storage. Their performance, however, is strongly influenced by operating conditions such as current density, temperature, and membrane transport properties. To study and optimise these effects, a zero-gap AEM electrolyser is modelled in Aspen Plus, and a parametric analysis is conducted to examine how various operating parameters affect cell voltage and overall system performance.

However, AEM is still an emerging technology, with ongoing challenges related to membrane conductivity, durability, and long-term stability.

To clearly highlight their differences, a comparison of key parameters, advantages, and disadvantages of AWE and AEM electrolysers is presented below:-

Table 1: Comparison Between AWE and AEM

Parameter	Alkaline Water Electrolyser (AWE)	Anion Exchange Membrane Electrolyser (AEM)
Electrolyte	Aqueous KOH (20–40 wt.%)	0–1 M KOH
Cathode	Ni, Ni–Mo alloys	Ni and Ni alloys
Anode	Ni, Ni–Co alloys	Ni, Fe, Co oxides
Separator	Diaphragm (≈500 μm)	AEM (20–100 μm)
Current density (A/cm²)	0.2–0.4	0.2–1.0
Cell voltage (V)	1.8–2.4	1.8–2.2
Operating temperature (°C)	60–80	50–60
Hydrogen purity	>99.5%	>99.99%
Technology status	Mature	R&D, emerging

Overall, while AWE remains a mature and low-cost technology, it continues to face several drawbacks, including the use of highly corrosive liquid electrolytes, gas crossover due to diaphragm-based separation, and limited current densities. These limitations make AWE less suitable for modern renewable-energy applications that require rapid load following and high gas purity. In contrast, AEM electrolysers offer a number of promising advantages that position them as an emerging alternative. Their solid polymer membrane significantly improves gas separation, enabling very reduced gas crossover, while the alkaline operating environment allows the use of inexpensive, non-noble metal catalysts. AEM systems are also

compatible with fluctuating power inputs from external sources, benefit from lower component costs. Despite challenges related to ionic conductivity and long-term membrane stability, the advantages of AEM technology—particularly in terms of cost, purity, and operational flexibility—highlight its strong potential for future hydrogen production systems.

Although AEM electrolysers have been modelled using a variety of simulation tools, their implementation in Aspen Plus remains largely unreported. Existing Aspen-based studies focus mainly on alkaline water electrolysers (AWE), whose voltage–current behaviour is described using semi-empirical relationships derived from the high-overpotential form of the Butler–Volmer equation. These formulations, which combine activation losses, ohmic resistance and logarithmic current dependence, are widely used for industrial alkaline systems and become applicable to AEM electrolysers as well under certain general conditions. Specifically, when the electrolyser operates in an alkaline environment, when hydroxide ions serve as the charge-carrying species, and when the cell is assumed to function in a zero-gap configuration that minimizes additional mass-transfer and interfacial resistances, the fundamental behaviour of a zero-gap AEM cell aligns closely with that of an alkaline electrolyser. Under these assumptions, the semi-empirical kinetic framework built into the Aspen AWE model can reasonably approximate the activation and ohmic characteristics of an AEM electrolyser.

Recognizing this compatibility, the present study adapts the AWE modelling structure available in Aspen Plus to construct a representative AEM electrolyser model. This enables a systematic parametric analysis to evaluate how operating conditions such as current density, temperature and membrane properties influence cell voltage and overall performance, helping address the existing gap in Aspen-based modelling studies for AEM electrolysis systems.

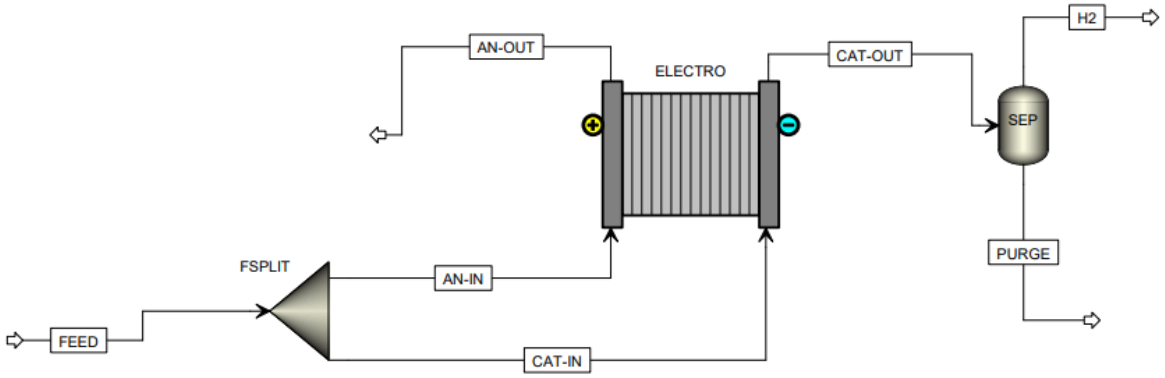

Figure 1: Aspen Simulation Used in This project

Objective:

1. To develop a zero-gap AEM electrolyser model in Aspen Plus by adapting the AWE mathematical framework under the assumptions of alkaline operation, hydroxide-ion conduction, and Tafel-type activation behaviour.

2. To perform a systematic parametric analysis to study the effect of temperature, current density, membrane thickness, and ionic conductivity on cell voltage and overall performance.

3. To apply the adapted AWE-based voltage expressions to AEM modelling and generate performance trends that can support understanding and optimisation of AEM electrolyser operation in Aspen Plus.

Theory:

1 Thermodynamics of Anion Exchange Membrane Electrolyser at pH 13

In an Anion Exchange Membrane Electrolyser, water is split into hydrogen and oxygen through two half-cell reactions. At pH 13, the reactions are written as:

Cathode (HER):

$$2H_2O + 2e^- \rightarrow H_2 + 2OH^- \quad \ldots(1)$$

Anode (OER):

$$2OH^- \rightarrow 1/2O_2 + 2H_2O + 2e^- \quad \ldots(2)$$

For pH = 13:

$$E^\circ_{\mathrm{HER}} = -0.769\ \mathrm{V}, E^\circ_{\mathrm{OER}} = +0.460\ \mathrm{V} \quad ..(3)$$

So the reversible cell voltage at 25 °C becomes:

$$E^\circ_{\mathrm{rev}} = 1.229\ \mathrm{V} \quad \ldots(4)$$

These values match those reported in alkaline electrolyser studies.

Temperature-Dependent Reversible Voltage:

The reversible voltage also depends on temperature. It comes from the Gibbs free energy change of the reaction:

$$E_{\mathrm{rev}} = \frac{\Delta G}{2F} = \frac{\Delta H}{2F} - T\frac{\Delta S}{2F} \quad \ldots(5)$$

The reference paper gives the following standard values:

$$\frac{\Delta H^0}{2F} = 1.481\ \mathrm{V}, \frac{\Delta S^0}{2F} = 0.000846\ \mathrm{VK^{-1}} \quad \ldots(6)$$

This gives a simple expression for the reversible voltage:

$$\boxed{E^0_{\mathrm{rev}} = 1.481 - 0.000846\,T_{\mathrm{cell}}} \quad \ldots(7)$$

This relation is used in the present model because the electrolyser runs at low pressure and with continuous water feed. Under these conditions, the gas activities stay close to 1, so no partial-pressure terms are needed.

2 Operating Principle of an AEM Electrolyser

An Anion Exchange Membrane (AEM) electrolyser operates using a solid polymer membrane that selectively conducts hydroxide ions (OH^-). The membrane contains fixed positively charged functional groups that attract and transport OH^- from the cathode to the anode. Water is supplied directly to both electrodes in a zero-gap configuration to maintain membrane hydration and to provide a constant reactant source.

At the cathode, water is reduced to hydrogen and hydroxide ions. The generated OH^- ions migrate through the AEM towards the anode under the influence of the electric field. At the anode, the hydroxide ions are oxidised to oxygen gas and water, releasing electrons that travel through the external circuit back to the cathode. The overall reaction corresponds to the decomposition of liquid water into hydrogen and oxygen.

The zero-gap arrangement minimises the ionic path length and reduces resistive losses, improving efficiency compared to configurations with a liquid electrolyte gap.

3 Activation Overpotential

Activation losses come from the energy barrier for reactions at each electrode. The full Butler–Volmer equation for each electrode is:

$$i = i_0 \left[\exp\left(\frac{\alpha_a z F \eta}{RT}\right) - \exp\left(-\frac{\alpha_c z F \eta}{RT}\right)\right] \quad \ldots(7)$$

However, water electrolysers usually operate at high overpotentials where one exponential term dominates. This leads to the simpler Tafel form:

Anode (OER):

$$\eta_a = \frac{RT}{\alpha_{a,a} F} \ln\left(\frac{i}{i_{0,a}}\right) \quad \ldots(8)$$

Cathode (HER):

$$\eta_c = \frac{RT}{\alpha_{c,c} F} \ln\left(\frac{i}{i_{0,c}}\right) \quad \ldots(9)$$

So the total activation overpotential is:

$$\eta_{\text{act}} = \eta_a + \eta_c \quad \ldots(10)$$

In alkaline media, the hydrogen evolution reaction (HER) proceeds through an initial water-dissociation step before molecular hydrogen can form, which makes the reaction inherently slow because the catalyst must first split H_2O to generate adsorbed hydrogen. The oxygen evolution reaction (OER), although involving multi-step electron-transfer and O–O bond-formation pathways on metal-oxide surfaces, benefits from the relatively high intrinsic activity of nickel-based oxides commonly used in AEM systems. As a result, HER on non-noble catalysts exhibits a much lower exchange current density than OER, leading to a larger cathodic activation overpotential. Local water depletion near the cathode can further slow HER under high current densities, whereas the anode typically has ample OH^- availability in zero-gap AEM designs, supporting more favourable OER kinetics.

The Aspen Plus AWE module employs a semi-empirical logarithmic activation expression equivalent to this Tafel form. Since AEM and AWE cells share the same alkaline HER and OER chemistry and operate in the Tafel region, the AWE activation formulation is applicable to AEM modelling.

4 Ohmic Overpotential

Ohmic losses mostly come from moving OH^- ions through the AEM membrane.
The membrane resistance is written as:

$$R_{i,\mathrm{mem}} = \frac{\delta_{\mathrm{mem}}}{\sigma_{i,\mathrm{mem}}\, A_{\mathrm{mem}}} \quad \ldots(11)$$

The total ohmic drop is:

$$\eta_{\mathrm{ohmic}} = i\, A_{\mathrm{cell}}\left(R_{i,\mathrm{mem}} + R_{\mathrm{assembly}}\right) \quad \ldots(12)$$

Here, i= current density, R_{assembly}= combined small resistances from electrodes and contacts.

5 Concentration Overpotential

A concentration or diffusion overpotential occurs when the gas concentration at the electrode interface differs from its standard value.
The expression used is:

$$\eta_{\mathrm{conc}} = \frac{RT}{4F}\ln\left(\frac{C_{\mathrm{O_2},m|e}}{C_{\mathrm{O_2},m|e,0}}\right) + \frac{RT}{2F}\ln\left(\frac{C_{\mathrm{H_2},m|e}}{C_{\mathrm{H_2},m|e,0}}\right) \quad \ldots(13)$$

In this work, the contribution of this term is minimal because water is continuously supplied to both electrodes, keeping the membrane well-hydrated, and the zero-gap cell configuration minimises diffusion distances. In addition, gas bubbles can easily escape through the porous electrode layers, reducing mass-transfer limitations, and the operating pressure is kept low, further suppressing concentration losses. As a result, the interfacial gas concentrations remain close to their standard values, and the logarithmic terms become nearly zero.

So for this model:

$$\eta_{\mathrm{conc}} \ll \eta_{\mathrm{act}} \text{ and } \eta_{\mathrm{ohmic}} \quad \ldots(14)$$

Methodology:

1. Model Formulation:

Adapting the AWE Framework for AEM Electrolysis:

The mathematical structure of an alkaline water electrolyser (AWE) was adapted for modelling the AEM electrolyser because both systems operate under alkaline conditions and share similar reaction mechanisms. The cell voltage was expressed as:

$$V_{\text{cell}} = E_{\text{rev}} + \eta_{\text{act}} + \eta_{\text{ohm}} + \eta_{\text{conc}} \quad \ldots(15)$$

Activation Overpotential: Activation behaviour was represented using Tafel-type kinetics, assuming charge-transfer control and operation in the moderate-to-high overpotential region. These activation effects were later incorporated through Aspen's semi-empirical logarithmic term.

Ohmic Overpotential: Ohmic losses were calculated from hydroxide-ion transport through the membrane. The membrane resistance is:

$$R_{\text{mem}} = \frac{\delta_m}{\kappa_{\text{AEM}} A_m} \ldots(16)$$

and the corresponding overpotential is:

$$\boxed{\eta_{\text{ohm}} = I \frac{\delta_m}{\kappa_{\text{AEM}} A_m}} \quad \ldots(17)$$

where, I— total cell current (A), A_m— active membrane area (m^2), δ_m— membrane thickness (m), κ_{AEM}— ionic conductivity of the AEM membrane ($S \cdot m^{-1}$)

Concentration Overpotential

Concentration losses due to reactant depletion and gas-bubble effects were included using Aspen's built-in mass-transfer expressions for alkaline electrolysis, which can be neglected.

Aspen Semi-Empirical Voltage Model

The AEM electrolyser voltage was implemented using an Aspen Plus empirical expression:

$$\boxed{V = E_{\text{rev}} + rI + s\ln(1 + tI)} \quad \ldots(18)$$

Where, E_{rev}— reversible thermodynamic voltage, rI— linear ohmic term, $s\ln(1 + tI)$— combined activation and concentration overpotential

The parameters r, s, and t were used as provided, since the empirical expression already reproduces Tafel-type behaviour that is consistent with both AWE and AEM electrolysers. Therefore, no additional tuning was required.

2. Model Implementation in Aspen Plus:

Developing the Zero-Gap Configuration: A single electrolyser block was configured in a zero-gap setup, with the electrodes directly contacting the membrane, and operated in a KOH-equivalent alkaline environment to mimic effective OH^- transport.

Table 2: Structural parameters and components set for AEM electrolyser

Parameter	Value
Cathode Active Area	1 cm^2
Anode Active Area	1 cm^2
Thickness of cathode electrode	250 µm
Thickness of anode electrode	250 µm
Membrane Active Area	9 cm^2
Thickness	60 µm
Stacks	1
Cells per stack	1
Reference cathode exchange current density	0.001
Reference cathode exchange current density	1e-5

Table 3: Operational parameter set-up for AEM electrolyser

Parameter	Value
Total current	0.6 A
Temperature of electrolyser	20 °C
Feed flow rate	1.56 ml/min
Concentration of KOH	0.1 M
Feed to anode ratio	0.5

A base-case simulation was run using the defined operating and structural parameters to confirm stable and realistic model behaviour. This base case served as the reference for the subsequent parametric analysis.

3. Parametric Analysis:

To understand the influence of key design and operating variables on the AEM electrolyser performance, a systematic parametric analysis was carried out in Aspen Plus. Each parameter was varied individually while keeping all other conditions at their base-case values.

Temperature: Cell temperature was varied to evaluate its effect on activation overpotentials. Higher temperature typically improves electrode kinetics and ionic conductivity, reducing the overall cell voltage.

Electrolyte (KOH-equivalent) Concentration: The AEM environment was simulated using equivalent alkaline concentration levels. This parameter affects the ionic conductivity of the electrolyte channels.

Membrane Thickness: Membrane thickness was systematically varied to quantify its influence on ionic resistance. Since the ohmic term is proportional to membrane thickness (δm), thinner membranes are expected to reduce voltage losses

Anode Exchange Current Density (OER Kinetics): The anode exchange current density was varied over several orders of magnitude to examine its effect on activation losses. This helps quantify how sensitive the model is to OER kinetics and the electrocatalyst activity.

Cathode Exchange Current Density (HER Kinetics): Similarly, the cathode exchange current density was adjusted to study the behaviour of hydrogen evolution kinetics. This reveals whether HER activation losses significantly contribute to the total voltage.

Result and Discussions:

1.Outlet flows and compositions (base case: I = 0.6 A, T = 20 °C, P=1 Bar)

Hydrogen (CAT-OUT):

- Vapor molar flow: 1.106×10^{-5} kmol h^{-1}
- Vapor mole fraction (gas purity basis): 0.9767 ≈ 97.7 % H_2

Oxygen (AN-OUT):

- Vapor molar flow: 5.506×10^{-6} kmol h^{-1}
- Vapor mole fraction (gas purity basis): 0.9688 ≈ 96.9 % O_2

Voltage and efficiencies:

- Cell voltage: 1.984 V at 0.6 A
- Voltage efficiency (Aspen): 0.747

Overpotential breakdown:

- Activation (total): 0.512 V (anode 0.198 V, cathode 0.313 V).
- Ohmic: 0.239 V.
- Concentration: 1.45×10^{-4} V (negligible).

2.Polarization Curve:

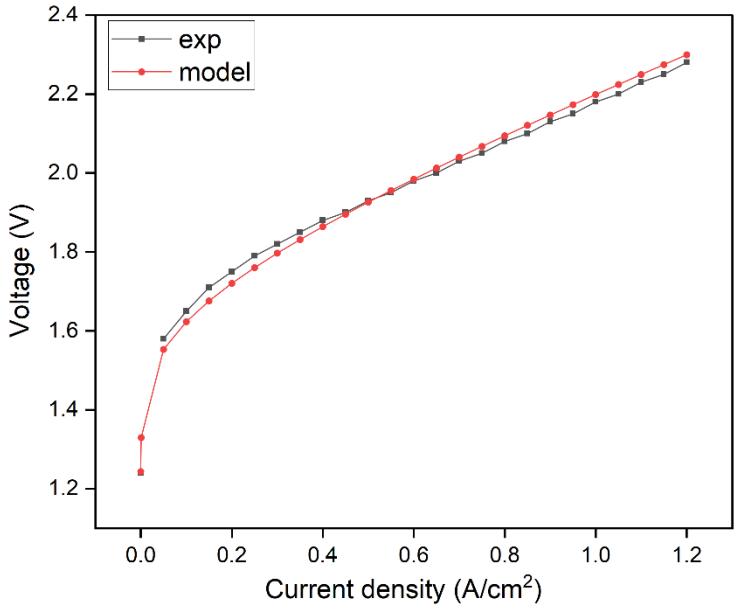

Figure 2:Experiment vs Model

The model shows excellent agreement with the experimental polarization curve(Nuggehalli Sampathkumar, 2024), reproducing both the activation-dominated voltage rise at low current densities and the linear ohmic-controlled region at higher currents. Minor deviations at very low currents are expected due to kinetic limitations not fully captured in the simplified activation term.

3. Overpotential Distribution:

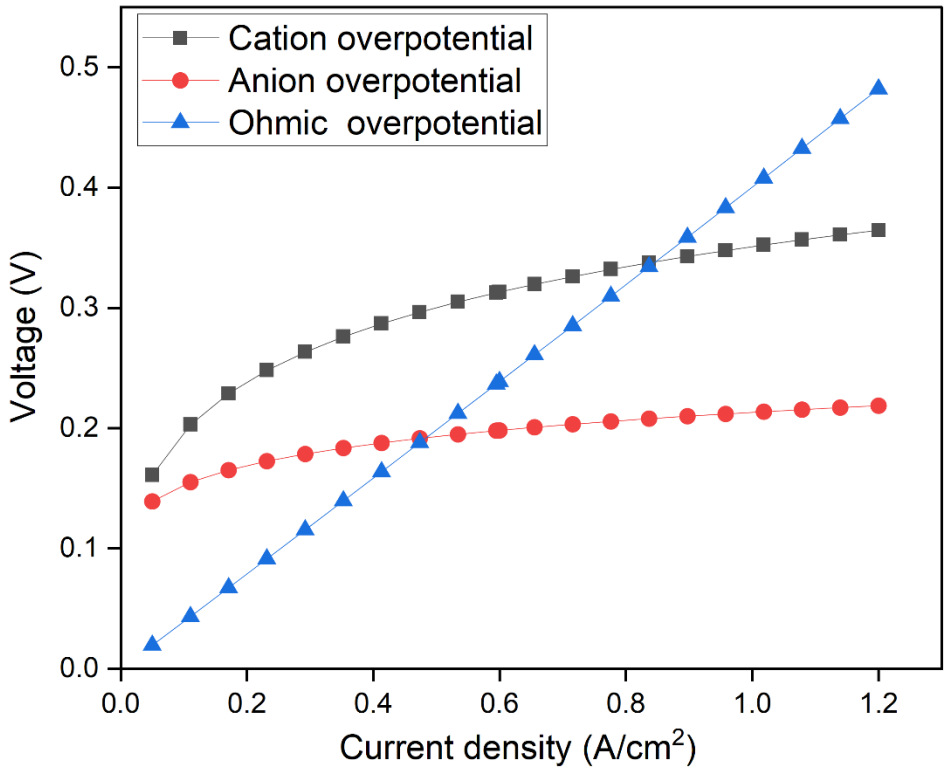

Figure 3: Analysis of overpotential effect in AEM electrolyzer

The figure shows how the different overpotentials vary with current density. The cation and anion overpotentials represent the activation losses at the cathode and anode, and both rise quickly at low current densities because the electrochemical reactions are slower in this region. The cation overpotential is higher because water is continuously consumed at the cathode during hydrogen evolution, and this makes the reaction more demanding and less kinetically favourable than the anode side. As a result, the cathodic reaction requires a larger driving force, leading to a higher cation overpotential across the operating range.

The ohmic overpotential, on the other hand, increases almost linearly with current density. This happens because the resistance of the membrane and electrolyte causes voltage losses that grow directly with current. At higher current densities, the ohmic overpotential becomes the dominant contributor to the total cell voltage.

In summary, the cell is mainly activation-controlled at low currents and becomes increasingly ohmic-controlled at higher currents.

4. H_2 Production and Voltage Efficiency vs Current Density:

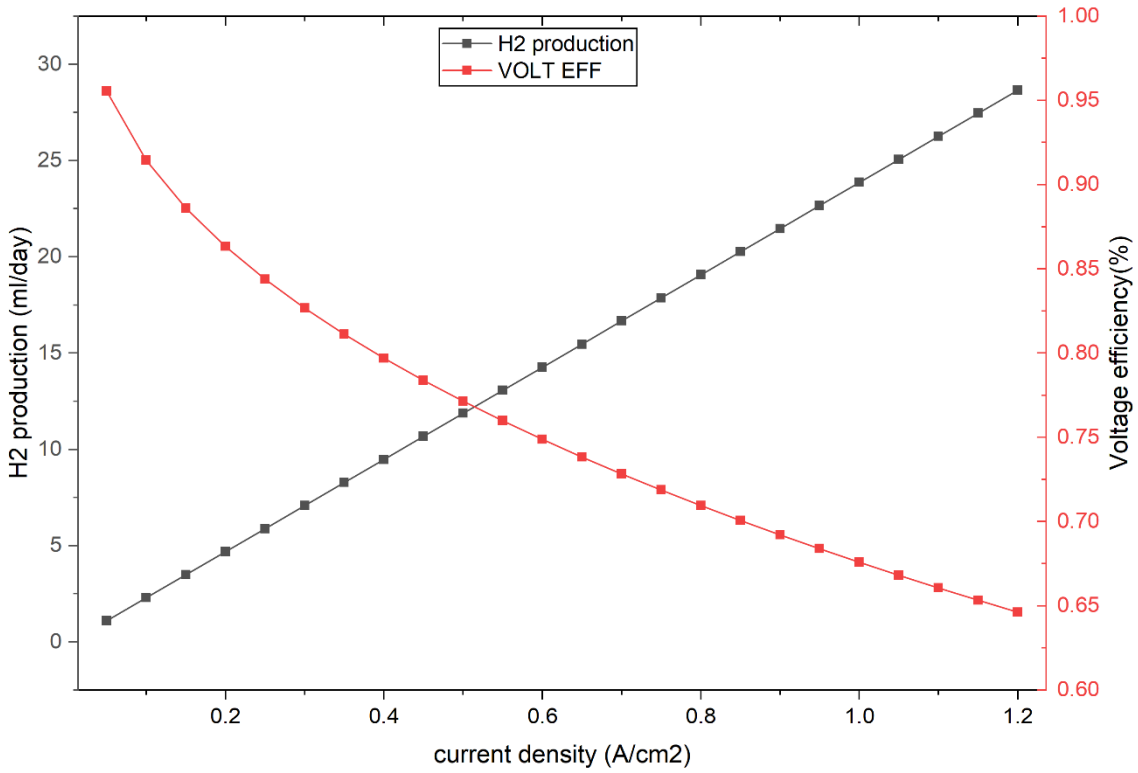

Figure 4:Analysis on voltage efficiency vs H2 production

The variation of the hydrogen production rate and voltage efficiency with current density. As expected, hydrogen production increases linearly with current density due to Faraday's law, since the rate of H_2 generation is directly proportional to the applied current. This linear rise indicates that the model maintains correct electrochemical stoichiometry and no mass-transfer limitations are present in the simulated operating range.

In contrast, the voltage efficiency decreases steadily with increasing current density. This decline occurs because the cell voltage rises more rapidly than the reversible voltage, mainly due to increasing activation and ohmic overpotentials at higher loads. At low current densities, where losses are minimal, the efficiency remains relatively high; however, as the current increases, the membrane's ionic resistance and electrode kinetics become dominant, leading to reduced efficiency.

The intersection of the hydrogen production and voltage efficiency curves occurs at approximately 0.52 A/cm². At this point, the voltage efficiency is around 77% which corresponds to the voltage of 1.87 V. The hydrogen production rate is approximately 12 mL/day. This operating condition represents a balanced "sweet spot," where the electrolyser delivers a reasonable hydrogen output while still maintaining acceptable voltage efficiency. Beyond this current density, hydrogen production continues to rise, but at the cost of a noticeable drop in efficiency.

5. Effect of Electrolyte Concentration on Polarization Behaviour:

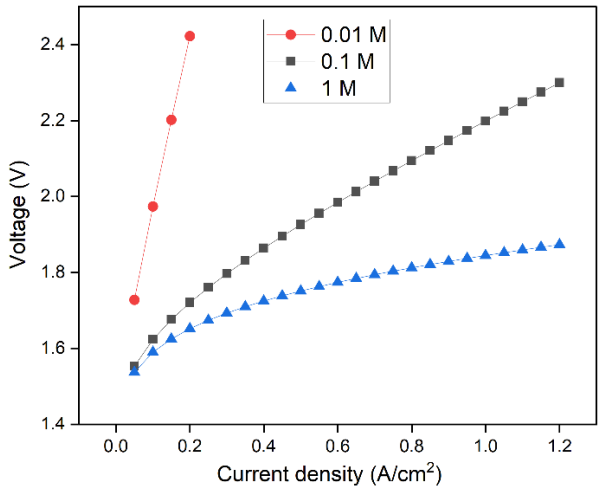

Figure 5: Effect of electrolyte concentration on AEM Electrolyzer

The figure shows the effect of electrolyte concentration on the polarization curve of the AEM electrolyser. As the KOH concentration increases from 0.01 M to 0.1 M and 1 M, the cell voltage decreases noticeably at the same current density. This trend occurs because a higher electrolyte concentration provides more ionic charge carriers (OH^- ions), which improves ionic conductivity and reduces the overall ohmic resistance of the cell. At very low concentrations such as 0.01 M, the shortage of OH^- leads to poor ionic transport and higher activation losses, causing the voltage to rise sharply even at small current densities. In contrast, 1 M KOH shows the lowest voltage across the entire range due to better ion mobility and more stable reaction conditions. Overall, increasing electrolyte concentration improves cell performance by reducing resistive losses and enabling smoother charge transfer during electrolysis.

6.Effect of Electrolyser Temperature on Polarization Behaviour:

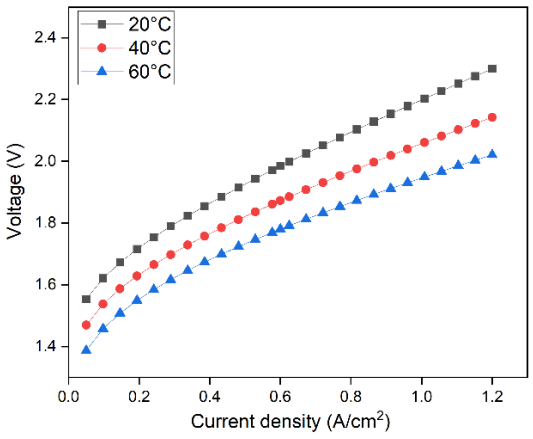

Figure 6: Analysis on Electrolyzer Temperature's effect on AEM electrolyzer

The results clearly indicate that the cell voltage decreases as the operating temperature increases. This behaviour occurs because higher temperatures improve electrode reaction kinetics and enhance ionic conductivity within the membrane and electrolyte. As a result, both activation losses and ohmic resistance become smaller at elevated temperatures, leading to lower voltage values for the same current density. The shift between 20°C and 40°C is significant, while the improvement from 40°C to 60°C is smoother but still noticeable. Overall, operating the electrolyser at higher temperatures improves performance by reducing internal voltage losses and enabling more efficient operation.

7. Effect of Membrane Thickness on Polarization Behaviour:

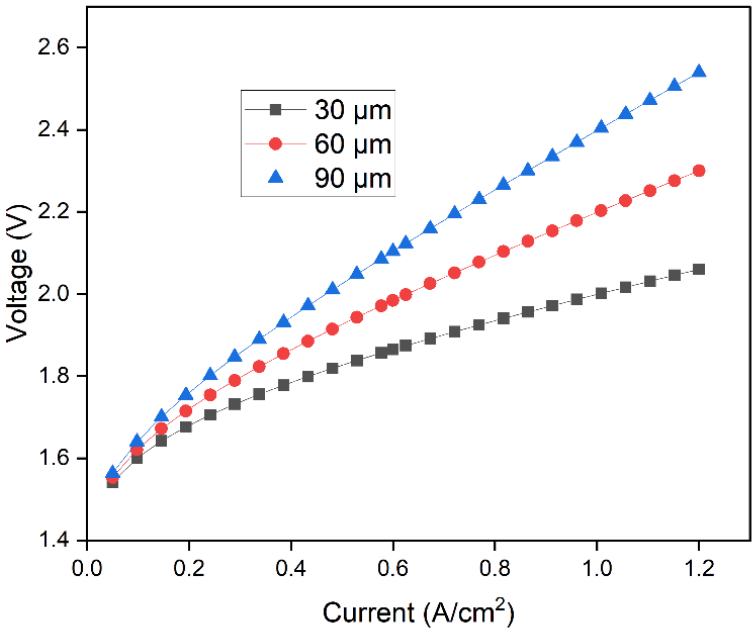

Figure 7: Effect of membrane thickness on AEM Electrolyzer

The results clearly demonstrate that the cell voltage increases as the membrane becomes thicker. This trend is mainly due to the increase in ionic transport resistance within the membrane. A thicker AEM provides a longer path for OH^- ions to travel from cathode to anode, which directly raises the ohmic overpotential. As a result, the 90 µm membrane exhibits the highest voltages across all current densities, while the 30 µm membrane consistently shows the lowest.

The separation between the curves becomes more noticeable at higher current densities, indicating that ohmic losses dominate in this region. Since OH^- conduction is the primary contributor to resistance in AEM cells, even moderate increases in membrane thickness significantly impact overall cell performance. Therefore, thinner membranes improve efficiency by minimising the internal voltage drop

8.Effect of feed flow rate:

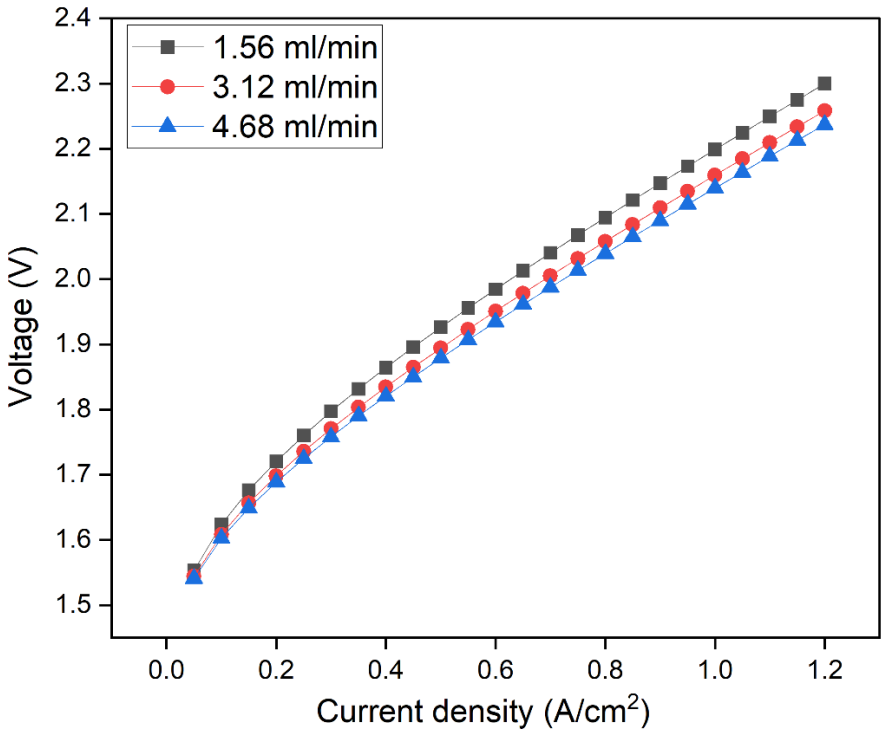

Figure 8: Effect of flow rate on AEM Electrolyzer

The first graph shows the polarization curves at three different inlet flow rates (1.56, 3.12, and 4.68 mL/min). All three curves almost overlap, with only a very small reduction in voltage at higher flow rates. This indicates that the flow rate has no meaningful effect on the cell voltage within this operating range. Since the electrolyser operates in a zero-gap configuration where water transport is dominated by membrane hydration and reaction consumption, increasing the bulk flow rate does not change the local reaction environment significantly.

Conclusion:

1. A complete zero-gap AEM electrolyser model was successfully developed in Aspen Plus by adapting the electrochemical framework of an alkaline water electrolyser (AWE). The modified voltage expression incorporated reversible voltage, activation losses, and membrane ohmic resistance.

2. The model accurately reproduced the experimental polarisation curve, showing close agreement across all current densities. This confirmed that the adapted AWE formulation is suitable for representing AEM electrolyser behaviour.

3. Temperature was found to be a major parameter affecting performance. Increasing temperature reduced the overall cell voltage due to improved electrode kinetics and enhanced ionic conductivity.

4. Electrolyte concentration (KOH-equivalent) strongly influenced ohmic behaviour. Higher concentrations lowered cell voltage by increasing the number of available OH^- ions for ionic transport.

5. Membrane thickness had a significant impact on ohmic resistance. Thinner membranes reduced the ionic path length, resulting in lower cell voltage throughout the current range.

6. Electrode exchange current densities influenced activation overpotentials. Both electrodes affected the activation region, with the anode (OER) showing a more noticeable sensitivity compared to the cathode (HER), indicating its stronger contribution to kinetic losses.

7. Feed flow rate did not produce any meaningful change in performance. Variations in inlet water flow did not alter the polarisation curve or hydrogen production under the studied conditions.

Future Work:

1. Scalability of the AEM Electrolyser System: Future work can extend the present single-cell model to a full stack-level simulation to investigate the scalability of AEM electrolysis. This includes analysing voltage balancing, heat distribution, membrane hydration management, and the impact of gas crossover at larger scales. A stack model would provide practical insights into commercial-scale operation and identify design limitations or optimisation opportunities relevant to industrial deployment.

2. A more detailed energy and process analysis should be carried out in Aspen to determine all external utilities required for the AEM electrolyser, including whether units such as heaters, coolers, pumps, or separators are needed for temperature control and product handling. A complete energy balance and assessment of heat-integration possibilities would clarify the system's overall energy demand. Additionally, the recyclability of the KOH solution should be examined, as electrolyte recovery can reduce chemical consumption and operating costs; incorporating a closed-loop KOH recycling scheme with suitable separation or purification steps would provide a more realistic and sustainable process representation..

References:

1. Lawand, K., Nuggehalli Sampathkumar, S., Mury, Z., & Van Herle, J. (2024). *Membrane electrode assembly simulation of anion exchange membrane water electrolysis*. Journal of Power Sources, 595, 234047.

2. Gunuru, M., & Paravada, M. (2025). *Mathematical modelling of an AEMWE: Investigating optimum operating conditions of an alkaline-fed AEM electrolyser.* International Journal of Hydrogen Energy, 50, 332550

3. An, L., Zhao, T. S. Chai, Z. H. Tan, P., & Zeng L. (2014). *Mathematical modeling of an anion-exchange membrane water electrolyzer for hydrogen production*. International Journal of Hydrogen Energy, 39(35), 19869–19876.

4. H. A. Miller , Bouzek K., Hnat, J., Loos, S., Bernäcker, C. I., Weißgärber, T., Röntzsch, L., & Meier-Haack, J. (2020). *Green hydrogen from anion exchange membrane water electrolysis: A review of recent developments in critical materials and operating conditions*. Sustainable Energy & Fuels, 4, 2114–2133.

5. Du, N., Roy, C., Peach, R., Turnbull, M., Thiele, S., & Bock, C. (2022). *Anion-exchange membrane water electrolyzers*. Chemical Reviews, 122(14), 11830–11895

.6. Ulleberg, Ø. (2003). *Modeling of advanced alkaline electrolyzers: A system simulation approach.* International Journal of Hydrogen Energy, 28(1–2), 21–33.

7. Aspen documentation on AWE electrolyzers.

8. Du, N., Roy, C., Peach, R., Turnbull, M., Thiele, S., & Bock, C. (2022). *Anion-exchange membrane water electrolyzers.* Chemical Reviews, 122(14), 11830–11895.

Nomenclature:

Symbol	Description
E°_{HER}	Standard electrode potential of the hydrogen evolution reaction (HER) at pH 13 (V).
E°_{OER}	Standard electrode potential of the oxygen evolution reaction (OER) at pH 13 (V).
E°_{rev}	Standard reversible cell voltage at 25 °C (V).
E_{rev}	Reversible cell voltage at operating temperature T_{cell}(V).
ΔG	Gibbs free energy change of the water-splitting reaction (kJ·mol^{-1}).
ΔH	Enthalpy change of reaction (kJ·mol^{-1}).
ΔS	Entropy change of reaction (kJ·mol^{-1}·K^{-1}).
ΔH^{0}	Standard enthalpy change at 1 bar, 25 °C (kJ·mol^{-1}).
ΔS^{0}	Standard entropy change at 1 bar, 25 °C (kJ·mol^{-1}·K^{-1}).
T_{cell}	Operating temperature of the electrolyser (K).
F	Faraday constant (96485 C·mol^{-1}).
i	Current density (A·m^{-2}).
i_{0}	Exchange current density (A·m^{-2}).
$i_{0,a}$	Anode exchange current density for the OER (A·m^{-2}).
$i_{0,c}$	Cathode exchange current density for the HER (A·m^{-2}).
η_{act}	Total activation overpotential (V).
η_{a}	Anodic activation overpotential (V).
η_{c}	Cathodic activation overpotential (V).
α_{a}	Anodic charge-transfer coefficient (–).
α_{c}	Cathodic charge-transfer coefficient (–).
z	Electron-transfer number (–); z=4for OER, z=2for HER.
η_{ohmic}	Ohmic overpotential (V).
$R_{i,\mathrm{mem}}$	Ionic area-specific resistance of the membrane (Ω·m^{2}).
R_{assembly}	Lumped resistance of electrodes, interfaces, and contacts (Ω·m^{2}).
δ_{mem}	Membrane thickness (m).

Symbol	Description
$\sigma_{i,\mathrm{mem}}$	Membrane ionic conductivity (S·m⁻¹).
A_{mem}	Membrane area (m²).
A_{cell}	Geometric active electrode area (m²).
η_{conc}	Concentration (diffusion) overpotential (V)
$C_{O_2,\mathrm{m\mid e}}$	Oxygen concentration at the membrane–electrode interface (mol·m⁻³)
$C_{O_2,\mathrm{m\mid e},0}$	Standard/reference oxygen concentration at the membrane–electrode interface (mol·m⁻³)
$C_{H_2,\mathrm{m\mid e}}$	Hydrogen concentration at the membrane–electrode interface (mol·m⁻³)
$C_{H_2,\mathrm{m\mid e},0}$	Standard/reference hydrogen concentration at the membrane–electrode interface (mol·m⁻³)